1-D COMPUTATIONAL MODEL OF A MOTIVE NOZZLE FOR THE R744 TWO-PHASE EJECTOR

K. BANASIAK[(A)], A. HAFNER[(B)], J. SMOLKA[(A)]
[(a)] Institute of Thermal Technology, Silesian University of Technology, Konarskiego 22,
Gliwice, 44-100, Poland
Fax: +48 32 237 28 72, e-mail: <krzysztof.banasiak@polsl.pl>
[(b)] SINTEF Energy Research, Kolbjørn Hejes v. 1D,
Trondheim, 7465, Norway
Fax: +47 73593950, e-mail: <armin.hafner@sintef.no>

ABSTRACT

The paper presents the results of a theoretical analysis performed for a motive nozzle of a two-phase R744 ejector at steady-state conditions. The model takes into consideration one-dimensional flow of real fluid through the converging-diverging nozzle. The proposed approach allows the determination of one-dimensional distributions of pressure, velocity and density. The simulated profiles take account of local values of the friction coefficient and physical properties of the working fluid, the latter based on the NIST database (REFPROP 8.0). Additionally, the approach allows the consideration of the metastable states of the fluid. The main practical advantage of the model is a possibility to assess the influence of both the geometry and operating parameters on the motive nozzle performance. The results derived from the numerical analysis were compared to the experimental measurements, performed at the test facility equipped with the two-phase ejector. The consistency between measured and simulated values was satisfactory.

1. INTRODUCTION

A proper design of a two-phase ejector for the expansion work recovery always requires a detailed analysis in terms of both numerical simulations and experimental work. Over the last 20 years much effort was put into development of computational codes capable of assessing the key features of the two-phase ejector/injector performance i.e. entrainment and pressure ratios along with the profiles of pressure, velocity and density. However, commercially available computational tools for mathematical modelling of the two-phase ejectors are still very limited. Therefore, the most advanced and appropriate computational techniques may be found among journal papers, where various approaches were presented, the form and complexity dependent on the objective of the research conducted.

The vast part of the scientific outcome concerned steady-state, 0-D or pseudo 1-D models of the ejection cycle, where the authors did not present any profile of thermal or transport properties. Balamurugan *et al.* (2006) provided and validated a 0-D semi-empirical model of a gas-water ejector, taking into account compressibility of air and the overall pressure losses of a two-phase mixture. Selvaraju and Mani (2004) and Nehdi *et al.* (2007) showed a design mode, pseudo 1-D (inlet/outlet conditions) theoretical analysis of the two-phase ejector cycle for several chlorofluorocarbons and hydrofluorocarbons. In their paper, the real fluid properties were calculated based on the REFPROP database. Cizungu *et al.* (2005) performed a pseudo 1-D design and off-design numerical analysis for the ammonia and ammonia-water two-phase ejectors. In addition, the authors optimised the ejector geometry to reach the maximum values for either entrainment ratio or pressure ratio. Lear *et al.* (2002) simulated choking conditions in a two-phase R134a ejector using pseudo 1-D equations of conservation for mass, momentum and energy, and equations of thermodynamic processes for the characteristic cross sections of the passage.

The authors of the mentioned papers took into account all the required geometrical parameters of the ejector along with the assumed integral coefficients like isentropic efficiencies for all the passages. As a result, they were able to perform an off-design analysis and to determine the operating characteristics of the ejector in this mode (Cizungu *et al.* 2005). However, the inlet-outlet structure of the governing equations which are non-linear algebraic equations for velocity, pressure, density, enthalpy and cross-section area of the duct is still a substantial drawback because the local field quantities cannot be evaluated.

In addition, none of the presented works included an analysis of the metastable conditions occurring during the phase transitions. As a consequence, the thermodynamic equilibrium was assumed for the entire two-phase region and the fluid was considered to be spatially homogenous. It means that all the conservation equations were formulated for the single-phase with the average-weighted properties, where the weighting factor was the equilibrium quality. Those limitations can be overcome by applying multidimensional, transient and heterogeneous fluid analysis of two-phase flows.

Städtke (2006) formulated general conservation equations for transient, 2-D flow of heterogeneous two-phase fluid. The governing equations included four pairs of main partial differential equations for mass, momentum, energy, and entropy defined separately for each phase. The author presented the results of numerous validating tests, performed for various cases of transient flows. For example, he showed the pressure wave propagation, the flow through convergent-divergent nozzles, the blowdown pipes, etc., for which the single-phase flow patterns were compared to the two-phase ones. Although the derived approach is very comprehensive and the obtained results are an absolute frontier research, the complexity of the model may cause some practical disadvantages when modelling ejector-like systems.

First, the transient form of the governing equations makes the computational process significantly longer. Since the ejecting systems perform their work mainly during relatively stable conditions, a steady-state formulation seems to be a reasonable and well-justified simplification. Second, multi-dimensionality of the problem should be reduced to reasonable extent, since at the modelling level it always leads to an additional growth of the computational time and considerable memory consumption. Unlike in the stream-mixing section cases, the expected profiles of velocity and thermal parameters for the converging-diverging nozzles demonstrate relatively low values of the radial gradient compared to the axial gradient (Städtke, 2006). Therefore, one may expect that the modelling of the motive/suction nozzle may be reduced to a 1-D problem without a significant loss of accuracy. Finally, a non-homogenous formulation of the two-phase fluid requires deep knowledge of the flow nature. In such an approach, the closure equations provide additional information about source terms as the interfacial mass, momentum and energy exchange between phases and body forces as the gravity. Moreover, those equations, are highly dependent on different two-phase flow pattern i.e. dispersed bubbly-droplet flow, annular flow, stratified flow, etc. Since the flow regime for the R744 two-phase ejectors has not been well analysed and reported yet, the homogenous flow model seems to be realistic approach for the current state of the knowledge. On the other hand, due to the nature of mathematical formulation of Städtke, the homogenous-fluid analysis would prevent the non-equilibrium state approach.

Attou and Seynhaeve (1999) presented a mathematical formulation for this kind of flow problems that was simultaneously sufficiently complex and on the other hand low-time consuming. Their 1-D model of the changeable cross-section area channel included non-equilibrium states, while the number of experimentally determined coefficients were kept at minimum. They solved the ordinary differential governing equations of mass, momentum and energy conservation for chemically uniform and spatially homogenous but evaporating/condensing two-phase fluid. The key feature of the code is the enthalpy-based energy conservation equation. In this formulation, the specific enthalpy is an independent variable in the axial coordinate, while the temperature is a function of the specific enthalpy and pressure. The approach utilised two alternative fluid models: Homogenous Equilibrium Model (HEM) and Delayed Equilibrium Model (DEM). The HEM model was based on the thermodynamic equilibrium for the entire two-phase region, while the DEM model introduced an additional fraction of the metastable liquid, gradually submitted to an isentropic flashing. Therefore, the model was supplied with only one closing equation in a form of additional total derivative for the metastable liquid fraction.

The objective of the present paper is to utilise the Attou and Seynhaeve approach for modelling of the two-phase R744 ejector motive nozzle and then to verify the closing equation for the metastable liquid fraction, since the correlation reported in the work of Attou and Seynhaeve was originally derived for the water condensate flashing in blowdown pipes. Although complex modelling of the two-phase ejectors requires much more effort to reliably reflect all the physical phenomena occurring downstream the ejector passages, the accurate numerical simulation of the motive nozzle performance is definitely crucial for the entire device. Therefore, as a first step to develop a complete simulation tool for the entire ejector modelling, solely a model for the motive nozzle was described in the paper. The presented model was experimentally validated based on the measurements of the ejector-equipped test facility.

2. MATHEMATICAL MODEL FORMULATION

The key assumptions made for the model formulations were as follows (Attou and Seynhaeve, 1999):

- The steady-state, one-dimensional flow of homogenous, chemically uniform and viscid two-phase fluid through a varying cross-section area, non-isothermal duct is considered (common mean values of density for both phases).
- There is a kinematical equilibrium between the liquid and gas phases (common mean values of velocity for both phases).
- The explicit effect of surface tension is neglected (common mean values of pressure for both phases).
- The effects of thermal diffusion and turbulence are not taken into account.
- The thermodynamic state of the two-phase fluid is modelled by DEM approach, where y denoting the mass fraction of the fluid transformed into saturated mixture of vapour and liquid is introduced as the 'vaporisation index'.

On the basis of the previous assumptions, the governing conservation equations for mass (Eq. (1)), momentum (Eq. (2)) and energy (Eq. (3)), along with the equation of state (Eq. (4)) may be represented as a system of ordinary differential equations:

$$\frac{1}{w}\frac{\mathrm{d}w}{\mathrm{d}l}+\frac{1}{A}\frac{\mathrm{d}A}{\mathrm{d}l}+\frac{1}{\rho}\frac{\mathrm{d}\rho}{\mathrm{d}l}=0 \tag{1}$$

$$A\frac{\mathrm{d}p}{\mathrm{d}l}+Aw\rho\frac{\mathrm{d}w}{\mathrm{d}l}+f\rho\frac{w^2}{2}\frac{\mathrm{d}F}{\mathrm{d}l}=0 \tag{2}$$

$$\frac{\mathrm{d}h}{\mathrm{d}l}+w\frac{\mathrm{d}w}{\mathrm{d}l}-\frac{k\left(T_{\mathrm{w}}-T\right)}{Aw\rho}\frac{\mathrm{d}F}{\mathrm{d}l}=0 \tag{3}$$

$$\left.\frac{\partial\rho}{\partial \mathrm{s}}\right|_p\frac{\mathrm{d}\mathrm{s}}{\mathrm{d}l}+\left.\frac{\partial\rho}{\partial p}\right|_{\mathrm{s}}\frac{\mathrm{d}p}{\mathrm{d}l}-\frac{\mathrm{d}\rho}{\mathrm{d}l}=0 \tag{4}$$

In the presented approach, the total derivatives of the pressure, velocity, specific enthalpy and density are set as the system unknowns. Then the total derivative of specific entropy $\frac{\mathrm{d}\mathrm{s}}{\mathrm{d}l}$ is replaced with the equivalent expression $\left(\frac{1}{T}\frac{\mathrm{d}h}{\mathrm{d}l}-\frac{1}{T\rho}\frac{\mathrm{d}p}{\mathrm{d}l}\right)$. As a result, Eqs (1)-(4) are transferred into the system of linear equations that can be written in an array notation:

$$\mathbf{\Omega}\cdot\mathbf{X}=\mathbf{B} \tag{5}$$

where the arrays $\mathbf{\Omega}$, $\mathbf{X}$ and $\mathbf{B}$ are defined as follows:

$$\mathbf{\Omega}=\begin{bmatrix} 0 & \frac{1}{w} & 0 & \frac{1}{\rho} \\ A & Aw\rho & 0 & 0 \\ 0 & w & 1 & 0 \\ \left.\frac{\partial\rho}{\partial p}\right|_{\mathrm{s}} & -\frac{1}{T\rho}\left.\frac{\partial\rho}{\partial \mathrm{s}}\right|_p & 0 & \frac{1}{T}\left.\frac{\partial\rho}{\partial \mathrm{s}}\right|_p & -1 \end{bmatrix} \tag{6}$$

$$\mathbf{X}^T=\begin{bmatrix}\frac{\mathrm{d}p}{\mathrm{d}l} & \frac{\mathrm{d}w}{\mathrm{d}l} & \frac{\mathrm{d}h}{\mathrm{d}l} & \frac{\mathrm{d}\rho}{\mathrm{d}l}\end{bmatrix} \tag{7}$$

$$\mathbf{B}^T = \left[-\frac{1}{A}\frac{\mathrm{d}A}{\mathrm{d}l} \quad -f\rho\frac{w^2}{2}\frac{\mathrm{d}F}{\mathrm{d}l} \quad \frac{k(T_\mathrm{w}-T)}{Aw\rho}\frac{\mathrm{d}F}{\mathrm{d}l} \quad 0 \right] \tag{8}$$

Solving Eq. (5) and introducing a general definition of the speed of sound $c = \sqrt{\left.\frac{\partial p}{\partial \rho}\right|_s}$, it yields:

$$\frac{\mathrm{d}p}{\mathrm{d}l} = \frac{T\left(A\mathrm{B}_1\rho - \frac{\mathrm{B}_2}{w^2}\right) + \left(\frac{\mathrm{B}_2}{\rho} - A\mathrm{B}_3\right)\left.\frac{\partial\rho}{\partial s}\right|_p}{AT\left(\frac{1}{c^2} - \frac{1}{w^2}\right)} \tag{9}$$

$$\frac{\mathrm{d}h}{\mathrm{d}l} = \frac{w^2(\mathrm{B}_2 - A\mathrm{B}_3\rho)\left.\frac{\partial\rho}{\partial s}\right|_p + T\rho\left(A\rho(w^2\mathrm{B}_1 - \mathrm{B}_3) + w^2(A\mathrm{B}_3\rho - \mathrm{B}_2)\frac{1}{c^2}\right)}{AT\rho^2w^2\left(\frac{1}{c^2} - \frac{1}{w^2}\right)} \tag{10}$$

$$\frac{\mathrm{d}w}{\mathrm{d}l} = \frac{w\left((A\mathrm{B}_3\rho - \mathrm{B}_2)\left.\frac{\partial\rho}{\partial s}\right|_p + T\rho\left(\mathrm{B}_2\frac{1}{c^2} - A\mathrm{B}_1\rho\right)\right)}{AT\rho^2w^2\left(\frac{1}{c^2} - \frac{1}{w^2}\right)} \tag{11}$$

$$\frac{\mathrm{d}\rho}{\mathrm{d}l} = \frac{(\mathrm{B}_2 - A\mathrm{B}_3\rho)\left.\frac{\partial\rho}{\partial s}\right|_p + T\rho(Aw^2\mathrm{B}_1\rho - \mathrm{B}_2)\frac{1}{c^2}}{AT\rho w^2\left(\frac{1}{c^2} - \frac{1}{w^2}\right)} \tag{12}$$

Both variables (p, h, ρ) and their functions (T, s) occurring in Eqs (9)-(12) take the average values for the two-phase region, where the weighting factors are mass fraction for the saturated gas x_g, mass fraction for the saturated liquid x_l and mass fraction for the metastable liquid x_m.
Given the definition of y,

$$y = \frac{m_\mathrm{l} + m_\mathrm{g}}{m_\mathrm{l} + m_\mathrm{g} + m_\mathrm{m}} \tag{13}$$

any specific parameter ϕ may be averaged as follows:

$$\bar{\phi} = x_\mathrm{m}\phi_\mathrm{m} + x_\mathrm{l}\phi_\mathrm{l} + x_\mathrm{g}\phi_\mathrm{g} = (1-y)\phi_\mathrm{m} + (y - x_\mathrm{g})\phi_\mathrm{l} + x_\mathrm{g}\phi_\mathrm{g} \tag{14}$$

Subsequently, partial derivatives of the averaged density $\bar{\rho}$ in Eq. (4) can be calculated in the following manner:

$$\left.\frac{\partial\bar{\rho}}{\partial p}\right|_s = \left(\frac{\bar{\rho}}{\rho_\mathrm{l}}\right)^2(y - x_\mathrm{g})\left.\frac{\partial\rho_\mathrm{l}}{\partial p}\right|_s + \left(\frac{\bar{\rho}}{\rho_\mathrm{g}}\right)^2 x_\mathrm{g}\left.\frac{\partial\rho_\mathrm{g}}{\partial p}\right|_s + \left(\frac{\bar{\rho}}{\rho_\mathrm{m}}\right)^2(1-y)\left.\frac{\partial\rho_\mathrm{m}}{\partial p}\right|_s \tag{15}$$

The derivative $\left.\frac{\partial\rho}{\partial s}\right|_p$ may be calculated analogically to the expression shown in Eq.(15).

The presented approach requires an additional closure equation for the vapourization index y. The following correlation was proposed originally by Féburie *et al.* (1993) and further tested in the works of Attou and Seynhaeve (1999), and García-Valladares (2007a and 2007b):

$$\frac{\mathrm{d}y}{\mathrm{d}l} = 0.02\frac{P}{A}(1-y)\left(\frac{p_{\mathrm{sat,l}} - p}{p_{\mathrm{cr}} - p_{\mathrm{sat,l}}}\right)^{0.25} \tag{16}$$

Therefore, the correlation was incorporated into the model. However, the right side of Eq. (16) was multiplied by a scaling factor C, which values were adjusted individually for R744 on the basis of the experimental results. The details of the verification procedure for the scaling factor are given in paragraph 3.
Thermal properties of the single-phase and equilibrium two-phase R744 were calculated according to the REFPROP 8.0 database, as well as the single-phase viscosity. The two-phase viscosity was approximated according to the Effective Medium Theory. This formulation was originally derived for the averaged thermal conductivity and successfully tested by Awad and Muzychka (2008) for the average viscosity of vapour-liquid mixtures for various refrigerants. The friction factor f in term B_2 was predicted by Churchill model (Churchill, 1977), while the pressure of vaporization onset at the flashing point was estimated with accordance to the correlation proposed by Chen *et al.* (1990). Properties of the metastable liquid were estimated by an extrapolation of properties for the saturated liquid at given pressure for both thermodynamic variables and their partial derivatives (Attou and Seynhaeve, 1999; García-Valladares, 2007a).

Eqs (9)-(12) and Eq. (16) were simultaneously integrated numerically by the fourth-order Runge-Kutta method and solved using an in-house Visual Basic for Application code.

3. VERIFICATION OF THE VAPORIZATION INDEX EQUATION

The verification procedure was based on the results of the experimental tests performed for the ejector-equipped R744 test facility. The examined motive nozzle geometry consisted of two conical ducts bored in a steel cylinder arranged in a converging-diverging channel. The main construction parameters were as follows:

- Diameters: 6 mm for the inlet cross-section, 1 mm for the throttle cross-section and 1.15 mm for the outlet cross-section,
- Angles of convergence: 30 ° for the converging section and -1 ° for the diverging section,
- Wall surface roughness: ca 1 μm for both sections assumed in accordance with the manufacturer.

The explicitly measured data reflecting the nozzle performance comprised the mass flow rate, the inlet pressure and the inlet temperature. Due to very small diameters of the motive nozzle passage, the motive nozzle cylinder encompassed by a suction chamber, it was impossible to directly measure any flow parameter downstream. Since the outlet cross-section was embedded inside the suction/mixing section passage, it was not feasible to register the exact value of the backpressure either. Hence, the inlet cross-section of the mixing section is the nearest spatially located point of pressure measurements (ca 2.5 mm), which may give only indicative but definitely not precise value of the backpressure.
The verification procedure comprised three levels of the inlet parameters for an approximately constant value of the mass flow rate (*Table 1*). It should be also noticed that all the tests were performed for the choking condition. It means that the registered mass flow rate represents the critical mass flow rate for the given geometry and operating conditions.

Table 1. The inlet parameters used for the model verification

Case number	Critical mass flow rate, kg/min.	Inlet pressure, bar	Inlet temperature, °C	Mixing section inlet pressure, bar
I	2.0±0.05	98.0±0.35	42.9±0.14	43.2±0.33
II	2.0±0.05	86.8±0.10	35.0±0.06	43.5±0.38
III	1.9±0.05	70.6±0.17	24.9±0.07	37.5±0.19

Numerical simulations (adiabatic expansion assumed for all cases) for case III approached the desired value of the critical mass flow rate within the range of measurement uncertainty for the scaling factor $C = 2000$, while in case II, this flow conditions were obtained for $C = 10000$. In the last case (Case I), the desired value was not reached even for the HEM model ($C \to +\infty$). The calculated values of the critical mass flow rate for case III were ca 7% higher than the values from the measurement (ca 5% above the uncertainty range).

The observed profile for the scaling factor C demonstrated significant dependence on the average level of the flashing pressure expressed as reduced pressure $\frac{p}{p_{cr}}$ were 0.809 for case III, 0.964 for case II and ~1 for case I, respectively. A physical explanation of the registered values may be delivered by a phase diagram analysis. The regions close to the critical point should be characterised by a smaller delay in a transition from the metastable to equilibrium conditions than the regions located far away from the critical point. The main reason is smaller surface tension effect preventing from equilibrium evaporation.

Therefore, in order to adapt Eq. (16) for the R744 ejector simulations, the following correlation for the scaling factor C was introduced into the model:

$$C = -\frac{\alpha}{\frac{p}{p_{cr}} - 1} + \beta \tag{17}$$

where $\alpha = 355.3$ and $\beta = 142$.

4. SIMULATION RESULTS

After the code adaptation for the transcritical R744 expansion processes, the model was validated comparing the results obtained from the numerical analysis and experimental measurements for five operating points with various mass flow rates (see *Table 2*). The calculations were performed for the self-adaptive grid, where the number of nodes was automatically adjusted in order to simultaneously fulfil two limiting conditions. First, the relative pressure change between nodes was not greater than the defined maximum value (typically 0.15%). Second, the number of nodes was greater than the defined minimum value (typically 400). Usually, the total number of nodes ranged between 700-900, which resulted in the reasonable computational times (approximately 5 minutes for a typical operating point using standard Pentium 4 CPU).

Table 2. Comparison of the results obtained from the numerical simulations (NS) and experimental measurements (EM)

Case	Inlet pressure, bar	Inlet temperature, °C	Critical mass flow rate			Back pressure (NS), bar	Expansion ratio (NS)	
			NS, kg/min.	EM, kg/min.	Relative discr.		1-phase range	2-phase range
1	79.9±0.30	35.1±0.14	1.494	1.50±0.05	−0.4%	29.1	1.094	2.514
2	74.4±0.26	30.0±0.05	1.729	1.70±0.05	1.7%	30.0	1.070	2.321
3	79.3±0.13	30.0±0.07	2.030	2.00±0.05	1.5%	34.1	1.184	1.963
4	82.8±0.12	30.0±0.05	2.311	2.23±0.05	3.6%	38.8	1.262	1.693
5	95.4±0.11	35.0±0.06	2.744	2.50±0.05	9.76%	48.0	1.390	1.429

An interesting remark derived from *Table 2* is the influence of the expansion line location on the relative discrepancy in the critical mass flow rate. The last two columns in *Table 2* show the simulated expansion ratio for both a single-phase and two-phase region. The total expansion ratio, defined as a ratio of the inlet pressure to the backpressure, is equal to the product of both partial ratios. The registered ratio of the single-phase expansion ratio to the total expansion ratio was as follows: 39.8% for Case 1, 43.1% for Case 2, 50.9% for Case 3, 59.1% for Case 4 and 70% for Case 5. Growing proportion of the single-phase expansion region evidently increased the critical mass flow rate discrepancy. Since for almost all examined cases the

flashing was practically entirely completed at the throttle due to high values the scaling factor C, all the phenomena occurring inside the two-phase section in the diverging cone of the nozzle do not influence the critical mass flow ratio. Therefore, the greater proportion of the two-phase expansion range is assumed, the smaller discrepancy is reported. This fact suggests either general slight underestimation of the friction factor for both ranges or too optimistic assumptions regarding the all surface roughness of the tested nozzle that was taken from the technical documentation delivered by the manufacturer. Both options are planned to be verified in the nearest future during the next stage of the research. Obviously, every correction of a correlation for the friction factor f shall be followed by a consecutive adaptation of the correlation for the scaling factor C.

The sample profiles of the pressure, Mach number and quality obtained in test 3 (see *Table 2 for the operating parameters)* prove that the model is also capable of a local, not only input-output analysis. An interesting observation derived from the local analysis concerned the spatial range of the flashing region that was below 0.5% of the total nozzle length for all the tested cases.

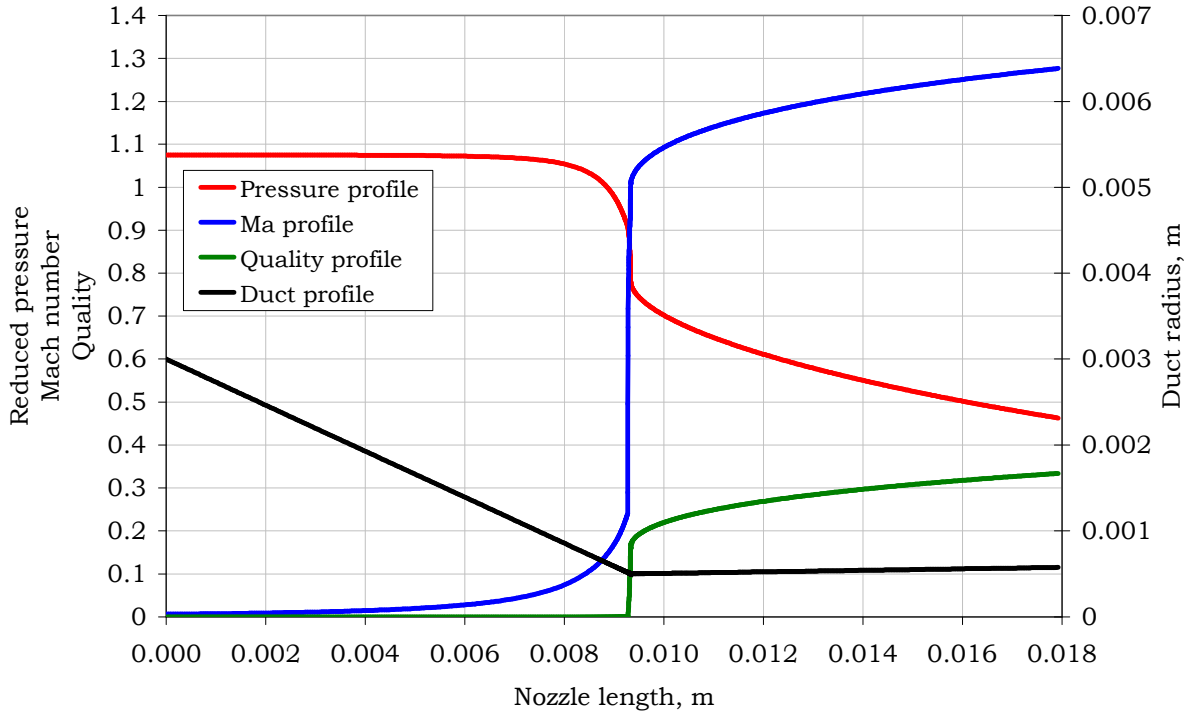

Figure 1. Profiles of the reduced pressure, Mach number and quality for the operating parameters listed in row 3 of *Table 2*

5. CONCLUSIONS

A one-dimensional DEM model was successfully utilised for the numerical simulation of the two-phase R744 ejector motive nozzle. The implemented self-adapting mesh ensured a satisfactory accuracy level while the computation procedure was relatively quick. The closing equation for the metastable liquid fraction was experimentally verified and adopted for the transcritical R744 expansion. The verification suggested very rapid, almost equilibrium, evaporation process inside the nozzle. This observation may be justified by high values of the reduced pressure over the flashing region for the tested operating conditions near the critical point plus relatively low values of surface tension for R744 compared to other refrigerants. The validation procedure for the critical mass flow rate registered the relative discrepancy values less than 10%, which should be considered as a satisfactory result. However, to improve an accuracy of the developed model, it will be adjusted in terms of the estimation of the friction factor values for both single-phase and two-phase regions.

NOMENCLATURE

Latin symbols

A	cross-section area, m^2
$\mathbf{B}$	constant terms vector in Eqs (5) and (8)
C	scaling factor for the left side of Eq. (17)
c	speed of sound, m/s
F	surface area of the nozzle wall, m^2
h	specific enthalpy, J/kg
k	heat transfer coefficient, $W/(m^2K)$
l	axial coordinate, m
m	mass, kg
P	wetted perimeter, m
p	pressure, Pa
s	specific entropy, J/(kgK)
T	temperature, K
w	velocity, m/s
$\mathbf{X}$	vector of unknowns in Eqs (5) and (7)
x	mass fraction
y	vaporization index

Greek symbols

α, β	coefficients in Eq. (17)
ϕ	any specific thermodynamic variable
ρ	density, kg/m^3
$\mathbf{\Omega}$	matrix of coefficients in Eqs (5) and (6)

Subscripts

cr	critical point value
g	gas phase
l	liquid phase
m	metastable phase
sat	saturated
w	wall

REFERENCES

1. Attuo A., Seynhaeve J.M. 1999, Steady-state critical two-phase flashing flow with possible multiple choking phenomenon. Part 1: Physical modelling and numerical procedure, *J. Loss Prevention in the Industries*, 12: 335-345.
2. Awad M.M., Muzychka Y.S. 2008, Effective property models for homogeneous two-phase flows, *Experimental Thermal and Fluid Science*, 33: 106-113.
3. Balamurugan S., Gaikar V.G., Patwardhan A.W. 2006, Hydrodynamic characteristics of gas-liquid ejectors, *Chemical Engineering Research and Design*, 84(A12): 1166-1179.
4. Chen Z.H., Li R.Y., Lin S., Chen Z.Y. 1990, A correlation for metastable flow of refrigerant 12 through capillary tubes, *ASHRAE Transactions*, 96 (1): 550-554.
5. Churchill S.W. 1977, Friction factor equation spans all fluid flow regimes, *Chem. Eng.*, 84 (24): 91-92.
6. Cizungu K., Groll M., Ling Z.G. 2005, Modelling and optimization of two-phase ejectors for cooling systems, *Applied Thermal Engineering*, 25: 1979-1994.
7. Féburie V., Giot M., Granger S., Seynhaeve J.M. 1993, A model for choked flow through cracks with inlet subcooling, *Int. J. Multiphase Flow*, 19: 541-562.
8. García-Valladares O. 2007, Numerical simulation of non-adiabatic capillary tubes considering metastable region. Part I: Mathematical formulation and numerical model, *Int. J. Refrigeration*, 30: 642-653.
9. García-Valladares O. 2007, Numerical simulation of non-adiabatic capillary tubes considering metastable region. Part II: Experimental validation, *Int. J. Refrigeration*, 30: 654-663.
10. Lear W.E., Parker G.M., Sherif S.A. 2002, Analysis of two-phase ejectors with Fabri choking, *J. of Mechanical Engineering Science*, Proc. Instn. Mech. Engrs, Vol. 216 (Part C): 607-621.
11. Nehdi E., Kairouani L., Bouzaina M. 2007, Performance analysis of the vapour compression cycle using ejector as an expander, *Int. J. Energy Research*, 31: 364-375.
12. Selvaraju A., Mani A. 2004, Analysis of an ejector with environment friendly refrigerants, *Applied Thermal Engineering,* 24: 827-838.
13. Städtke H. 2006, *Gasdynamic Aspects of Two-Phase Flow*, WILEY-VCH GmbH & Co. KGaA, Weinheim.